Forest Service
U.S. DEPARTMENT OF AGRICULTURE

Pacific Southwest Research Station | Research Note PSW-RN-428 | September 2025

Site-Sensitive Density Management Diagrams for Even- and Uneven-Aged California Mixed-Conifer Stands

Christopher Looney

Author

Christopher Looney is a research forester, U.S. Department of Agriculture, Forest Service, Pacific Southwest Research Station, 430 G Street, Davis, CA 95616.

Cover photo: Fog in a northern California forest. Photo by Trevor McBroom, stock.adobe.com.

Abstract

Looney, Christopher. 2025. Site-sensitive density management diagrams for even- and uneven-aged California mixed-conifer stands. Res. Note. PSW-RN-428. Vallejo, CA: U.S. Department of Agriculture, Forest Service, Pacific Southwest Research Station. 23 p. https://doi.org/10.2737/psw-rn-428.

Density management diagrams (DMDs) are a fundamental forest management tool. However, these tools were primarily developed for even-aged stands and may not incorporate important site effects. Accommodating different stocking constraints during stand development across broad ranges of site effects could help tailor reforestation and thinning prescriptions to local conditions. For that purpose, this report introduces a set of site-sensitive DMDs for managing both even- and uneven-aged California mixed-conifer stands. By consulting maps of aridity and nitrogen deposition summarized by California seed zone, users can match the appropriate DMD to their local site conditions. In addition to more detailed stocking guidelines, the diagrams also include features for estimating treatment scheduling and yield. I also provide management considerations for current conditions of frequent drought, elevated bark beetle activity, and wildfire risk.

KEYWORDS:
Density management diagram
Stand density index
California mixed-conifer
Maximum size-density line
Uneven-aged management
Reforestation

Contents

Introduction

The DMD is a foundational tool of silviculture, particularly in the Western United States. These diagrams allow foresters to anticipate tradeoffs between the number of trees per acre and the performance of individual trees. Foresters can use these simple graphical tools in both the field and the office to assess whether stands meet thresholds of minimal stocking, potential for maximizing stand-level growth, and the onset of density-dependent mortality (Ray et al. 2023). All these thresholds are defined relative to a maximum size-density line, analogous to carrying capacity, for a given forest type. DMDs are most commonly based on Reineke's (1933) stand-density index (SDI), which is derived from a predictable tradeoff between mean tree size and number of trees. This tradeoff makes it possible to express a wide range of stand structures on one common basis: the number of 10-inch diameter at breast height (DBH) tree equivalents per acre. An advantage of this metric is that stocking standards can be derived from basic forest inventory data, minimizing field data collection needs. Two historical limitations of DMDs have been (1) a restricted application to stands with even-aged structures and (2) limited ability to incorporate local site characteristics, such as aridity and soil fertility, that may restrict maximum tree stocking.

DMDs have primarily focused on even-aged monocultures characterized by bell-shaped DBH distributions. Under these conditions, quadratic mean diameter (QMD) can accurately represent the mean tree size on a DMD. Yet foresters commonly face more complex situations, such as uneven-aged management, restoring stands suffering from fire-intolerant conifer establishment, or maintaining mature and old-growth stands. Another complication is that complex, older stands may warrant different stocking guidelines compared to small-diameter, even-aged stands. Forest types worldwide show evidence of nonlinearity in the log-linear size-density relationship at high mean stand diameters (Forrester et al. 2021, Shaw and Long 2007).

Historically, DMDs have provided a single set of stocking guidelines for use across both low- and high-quality sites of a given forest type. However, advances in data and statistical analysis are making it possible to establish guidelines tailored to local conditions. Maximum stocking is commonly more limited on arid sites or poorer soils (Forrester et al. 2021, Kimsey et al. 2019). Maximum stocking may also vary with nitrogen deposition (Ndep) (Looney and Shaw 2025), a widespread form of air pollution that may have fertilization effects on forests at low to moderate intensities but has deleterious effects on soil nutrition and plant species composition at chronic levels (Schmitz et al. 2019). The challenges of aridity and air pollution, both of which can interact with stand development to complicate maturity-driven changes in maximum stocking, warrant new guidelines that are more specific to local stand and site conditions. Developing guidelines based on direct indicators of site quality is preferable to using site index, given the difficulties with quantifying site index for uneven-aged and mixed-species stands (Skovsgaard and Vanclay 2008).

The DMDs (app. 2), maps (app. 1), and supporting figures in this report enable managers to apply the results of Looney and Shaw (2025) to manage structurally complex stands of the California mixed-conifer forest type. This set of tools uses a set of five DMDs to illustrate how key management thresholds simultaneously vary under both aridity and low to moderate Ndep. These DMDs also display supplementary information for estimating treatment scheduling and stand volume.

Building the Diagrams

The DMDs, maps, and figures included here are an extension of the research, findings, and equations detailed by Looney and Shaw (2025). That study queried U.S. Department of Agriculture, Forest Service, Forest Inventory and Analysis (FIA) conditions, or stands, for the California mixed-conifer forest type—FIA forest type code 371 (Burrill et al. 2024) (see fig. A1.1). This forest type is comprised of a range of conifer species including ponderosa pine (*Pinus ponderosa* Lawson & C. Lawson), Jeffrey pine (*Pinus jeffreyi* Balf.), sugar pine (*Pinus lambertiana* Douglas), Douglas-fir (*Pseudotsuga menziesii* (Mirb.) Franco), white fir (*Abies concolor* (Gord. & Glend.) Lindl. ex Hildebr.), California red fir (*Abies magnifica* A. Murray bis), incense cedar (*Calocedrus decurrens* (Torr.) Florin), and giant sequoia (*Sequoiadendron giganteum* (Lindl.) J. Buchholz). Associated hardwoods include California black oak (*Quercus kelloggii* Newberry), tanoak (*Notholithocarpus densiflorus* (Hook. & Arn.) P.S. Manos, C.H. Cannon, & S.H. Oh), and bigleaf maple (*Acer macrophyllum* Pursh). The FIA California mixed-conifer forest type is defined as California stands comprised of at least 70 percent coniferous species and (1) otherwise falling into the sugar pine or incense cedar forest types (2) otherwise falling into the ponderosa pine, Jeffrey pine, white fir, or California red fir forest types but containing less than 80 percent relative basal area of their namesake species, and (3) falling into the Douglas-fir forest type in California counties besides Del Norte, Humboldt, Marin, Mendocino, Napa, San Mateo, Santa Clara, Santa Cruz, and Sonoma (Burrill et al. 2024).

I filtered the California mixed-conifer stands for those with >80 percent combined relative basal area of the principal conifer tree species listed above, no recent treatment history, and with at least two plot visits to examine change over time. I only used data from the most recent plot visit to avoid issues with the nonindependence of repeated measurements. FIA plots may sample multiple conditions, or stands, which may introduce extreme per-area estimates if only a small portion of plot area overlaps with a given stand. To avoid extreme per-acre estimates introduced by small sampled areas, I set another requirement that selected stands overlap with >50 percent of the FIA macroplot (58.9 foot-radius plots used to assess large trees) and >50 percent of the FIA microplot (6.8 foot-radius plots used to assess saplings) sampled area. Selected stands had a minimum Reineke's diameter (see below) of 2 inches and a minimum density of 25 trees per acre. I dropped one extreme outlier stand with a Reineke's diameter >31 inches. In contrast to the original analysis of Looney and Shaw (2025), I converted this model to U.S. standard units to yield trees per acre as the predicted response and included the additional constraint of a minimum of four stems per sampled stand to further protect against extreme per-acre estimates. Individual-tree records were expanded to stand-level estimates (Burrill et al. 2024). I used the FIESTA package version 3.7.1 (Frescino et al. 2023) to query and compile the FIA database from within the R statistical environment (R Core Team 2025).

I joined downscaled historical climate records for the 1991–2020 period (Wang et al. 2016) to FIA stand data based on public FIA plot coordinates and elevations. I also joined stand data to total wet + dry Ndep estimates averaged over the 2001–2020 period (Schwede and Lear 2014). I joined Ndep estimates to plot coordinates using bilinear interpolation in the raster package version 3.6 (Hijmans et al. 2025) for R. Compared to exact FIA coordinates, public FIA coordinates are shifted, or fuzzed, by about 800 meters (2,625 feet) on public lands. For added confidentiality, 20 percent of plots on private lands are also swapped with nearby similar plots and thus those locations are approximate to the county level (Burrill et al. 2024).

Considering the amount of public land in California and accuracy of the gridded data products, the added uncertainty from using publicly available coordinates typically has minimal effects on this style of analysis (Gibson et al. 2014).

Density management research commonly analyzes scatterplots of a mean stand diameter, typically QMD, versus trees per acre. In this study, I use Reineke's diameter as an alternative to address the shortcomings of QMD when applied to complex stands (Yang and Brandeis 2022). Reineke's diameter is calculated as follows:

$$Reineke's\ diameter = \left[(1/N)\sum D_i^{1.605}\right]^{1/1.605}$$

Where *N* is the total number of trees per acre in the stand, *D* is the DBH of individual-tree *i,* and 1.605 is Reineke's traditional exponent for SDI. In even-aged stands, Reineke's diameter and QMD will be roughly equivalent. Reineke's diameter will decline relative to QMD as DBH distributions become increasingly right-skewed or reverse-J shaped (Ducey and Larson 2003). These DMDs built using Reineke's diameter can therefore be applied to both even-aged and uneven-aged stands.

I estimated maximum stocking, as represented by maximum size-density lines, using multiple 0.95 quantile regression modeling (Koenker and Bassett 1978). This technique is one of several used in contemporary density management research (Chivhenge et al. 2024), but for this report, it has the key advantages of (1) making inferences about a specific quantile of site covariate (Tian et al. 2021), and (2) not masking stand development effects that are often considered nuisance factors in density management research (Weiskittel and Kuehne 2019) but are of prime interest for refining management guidelines for different stand development stages. The model presented here regressed trees per acre as a quadratic polynomial function of Reineke's diameter, in addition to the main effects or interactions with aridity and Ndep covariates, based on the results of Looney and Shaw (2025). I performed quantile regression analysis with version 6.1 of the quantreg package (Koenker et al. 2025) for R version 4.40 (R Core Team 2025).

I based DMDs on the two plausible 0.95 quantile regression models of the maximum size-density line for the California mixed-conifer forest type reported by Looney and Shaw (2025). I averaged these models in the MuMIn package version 1.48.11 (Bartoń 2025) using Akaike's information criterion weights (Burnham and Anderson 2002). These models fitted the maximum size-density line as quadratic polynomial functions of Reineke's diameter and aridity and Ndep covariates. Both models included a main effect of aridity, as indicated by the annual heat-moisture index (AHM) (Wang et al. 2016). This index is formulated as follows:

$$AHM = (MAT + 10)/(MAP + 1000)$$

Where *MAT* is mean annual temperature (ºC), and *MAP* is mean annual precipitation (millimeter/year).

In the first-ranked model (weight = 0.85), AHM acted as a main effect, with lower (more humid) values raising the maximum size-density line and higher (more arid) values lowering the maximum size-density boundary. The first-ranked model also included the main effect and interactions of Ndep with Reineke's diameter. These interactions allowed Ndep to alter the slope and curvature of the maximum size-density line. Under low Ndep rates (low air pollution), the maximum size-density line was more linear. Under higher Ndep rates (greater air pollution), the line was more strongly curvilinear, restricting maximum stocking for both small- and large-diameter stands, while promoting higher maximum stocking in intermediate-diameter stands. In the second-ranked model (weight = 0.15), curvature was contingent on AHM, while varying with the main effect of Ndep. In the second-ranked model, the curvature of the maximum size-density line became more pronounced as aridity declined, while the intercept, and by extension, overall stocking, increased with the main effect of Ndep. Considering the stronger support for the first-ranked model, the second-ranked model had comparatively minor influences on predicted maximum size-density lines.

In addition to determining maximum stocking, DMDs also incorporate estimated top height and live total volume for plotting on the DMDs. These details allow foresters to make rough estimates of treatment scheduling (Dean and Baldwin 1996), stand volume, and by extension, stand biomass and carbon. I quantified top height using Lorey's height, a basal area-weighted mean tree height (Husch et al. 2002) that is commonly assessed through prism or LiDAR surveys (Næsset 1997), as the metric of top height:

$$Lorey's\ height = \frac{\sum_i BA_i\, Ht_i}{\sum_i BA_i}$$

Where BA_i and Ht_i are the basal area and height of individual-tree *i*, respectively. Lorey's height provided a more logical metric of top height because other traditional metrics, such as the height of the tallest 40 trees per acre, lose meaning in the large-diameter, open stands included in this analysis. Volume is the sound cubic-foot volume of all live trees measured at the most recent plot visit.

I analyzed top height and volume as functions of trees per acre and Reineke's diameter using generalized linear mixed modeling. Given the sharp right-skew of these positive data, models include a log-link to the gamma error distribution. I performed generalized linear modeling in version 1.1.12 of the glmmTMB package (Brooks et al. 2025). I inspected simulated residuals plots (Hartig 2024) to verify model assumptions of homoscedasticity, the appropriateness of error distributions, and linear predictor-response relationships (e.g., Zuur et al. 2009). These diagnostics and comparisons of preliminary models prompted modeling both top height and volume as simple linear functions of log-transformed trees per acre and log-transformed Reineke's diameter. Collinearity was low-moderate (variance inflation factors <5) (Zuur et al. 2009).

Map Summaries of Historical Aridity and Ndep

Maps summarize AHM and Ndep values for quick reference when selecting the appropriate DMD and stocking guidelines to match local conditions (see figs. A1.2–A1.4). I summarized gridded data to the level of California seed zones (Buck et al. 1970, CAL FIRE 2023) based on estimates for FIA conditions located in each seed zone. The use of seed zones avoids the need for users to go through the complex process of estimating AHM and Ndep for their stand locations. Many users will already be familiar with their local seed zones through reforestation projects. AHM and Ndep estimates integrate California mixed-conifer FIA conditions as well as Douglas-fir, ponderosa pine, Jeffrey pine, white fir, and California red fir FIA forest type conditions. While the inclusion of data from other forest types did not substantially alter seed zone-level means, these additional data expanded the map to adjacent seed zones that were not sampled in the main analysis but may nevertheless contain the California mixed-conifer forest type.

Steps for Using the Diagrams

1. Determine the most applicable AHM and Ndep values for the stand based on the seed zone maps in appendix 1 (see figs. A1.2–A1.4). When matching mapped values in figures A1.3 and A1.4 with the DMDs in appendix 2, rounding up AHM and Ndep values will yield more conservative maximum stocking estimates.

2. Select the appropriate DMD based on the closest AHM value (see figs. A2.1–A2.5). Diagrams correspond to AHM values of 10, 15, 20, 25, or 30. While some seed zone means exceed this range of values, such extremes are uncommon in the data and represent <10th- and >90th- percentile cases.

3. Calculate trees per acre; include saplings (1.0–4.9 inches in DBH) to maximize compatibility with the DMDs.

4. Calculate Reineke's diameter for plotting stands on the DMD, including sapling data if available. Reineke's diameter can be calculated in two different ways:

4a. Based on individual trees or tallies of trees by DBH class:

$$Reineke's\ \ diameter = \left[(1/N)\sum D_i^{1.605}\right]^{1/1.605}$$

Where N is the total number of trees per acre in the stand, D is the DBH of individual-tree i, and 1.605 is Reineke's traditional exponent for SDI. For forest inventory or cruise data using different-sized plots by tree size class, expand the individual D_i values by the appropriate plot expansion factors. Both saplings and pole/sawtimber-sized trees should be included for maximum compatibility with the diagram.

4b. Based on trees per acre plus the summation, additive, or Zeide's version of SDI (Ducey and Larson 2003). Users can obtain Zeide's SDI via the FVS_Summary in the Forest Vegetation Simulator using the SDICALC keyword (Van Dyck and Smith-Mateja 2024). Zeide's SDI (Zeide 1983) can be manually calculated based on trees per acre (TPA) and individual-tree contributions to SDI (Ducey and Larson 2003):

$$Zeide's\ SDI = \sum\left(TPA_i * \left(\frac{D_i}{10}\right)^{1.605}\right)$$

Where TPA_i is the trees per acre represented by individual tree record *i,* and D_i is the diameter of individual tree record *i*. After obtaining TPA and Zeide's SDI, users can estimate Reineke's diameter using the following formula:

$$Reineke's\ diameter = 10 * \left(\frac{Zeide's\ SDI}{TPA}\right)^{1/1.605}$$

5. Find the appropriate set of density management guidelines by rounding to the nearest Ndep value. Plotted sets of guidelines correspond with Ndep rates of 2, 4, 6, or 10 kilograms of N/hectare/year. Ndep is coded by color, with brighter colors signifying heavier rates (figs. A2.1–A2.5).

6. Assess where stands fall relative to density management guidelines. Guidelines for different management zones in figures A2.1–A2.5 are depicted by line style. Moving from bottom to top and left to right on each diagram in appendix 2, the first set of guidelines marks the approximate onset of crown closure and inter-tree competition (25 percent of relative density). The second set of guidelines denotes the lower threshold of full site occupancy and potential for rapid tree growth (35 percent of relative density). The third set of guidelines represents the onset of imminent competition-related mortality (60 percent of relative density). The interval between the second and third sets of guidelines represents the traditional density management zone, which balances rapid stand growth against mortality risk. The fourth set of guidelines represents the maximum size-density line (100 percent of relative density), or maximum carrying capacity.
7. Optionally, users can reference the top height isolines, along with information on total stand age and a site index curve, to schedule thinning treatments. Top height isolines are labeled with leader lines and corresponding values. Figure 1 shows a set of California mixed-conifer site index curves with a base age (the common age at which height is indexed) of 50 years from Dunning and Reineke (1933). Note that site index will be unreliable in true uneven-aged stands where most trees have a history of suppression (Skovsgaard and Vanclay 2008). Also, stand age that is estimated based on breast-height age should account for the time trees need to reach 4.5 feet in height. For example, consider a California mixed-conifer stand reforested at a density of 200 trees per acre on a humid, low-pollution site with an AHM of 10 (fig. A2.1). Using figures 1 and A2.1, if site index = 90, this stand is expected to reach a relative density of 35 percent, a top height of about 70 feet, and warrant commercial thinning at an age of 35 years. When site index = 50, it would take 70 years to reach the same threshold for commercial thinning.

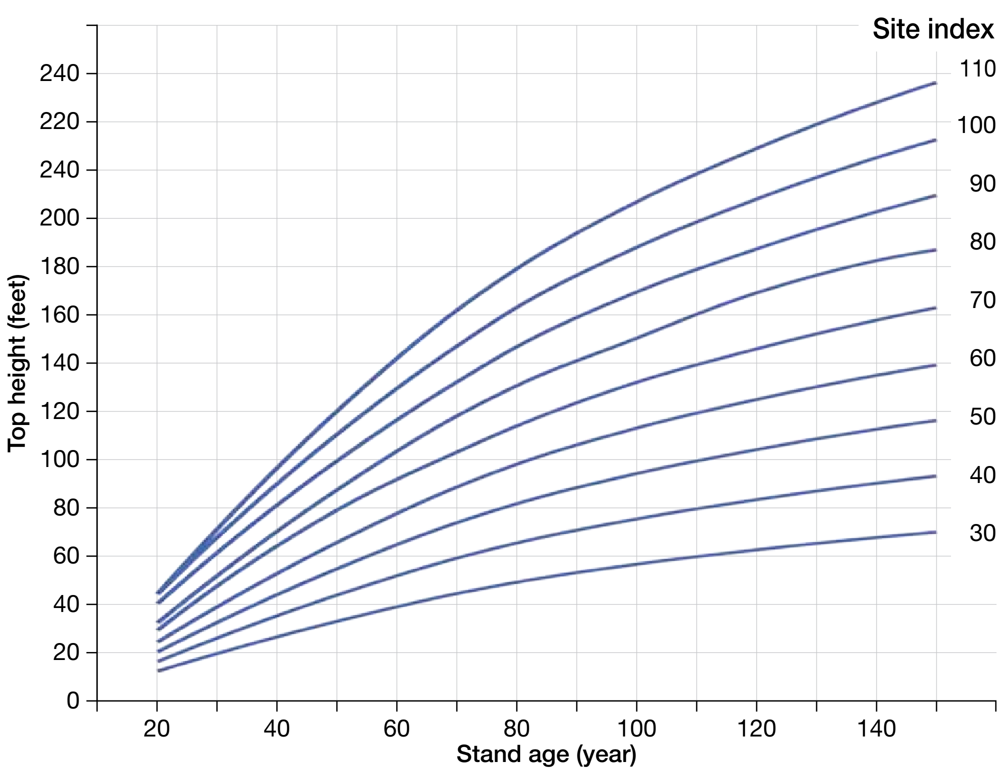

Figure 1—Site index curves for the California mixed-conifer forest type, based on a total tree (from seedling establishment) base age (the common age at which height is indexed) of 50 years, adapted from Dunning and Reineke (1933). Users can estimate treatment scheduling by cross referencing density management diagram top height lines at key condition thresholds, then finding the stand age corresponding to a given top height-site index combination in this chart.

8. Optionally, users can estimate total volume for various stand structures by reading the volume isolines; cubic-foot volume isolines are labeled with leader lines and corresponding values. For example, a stand with 200 trees per acre and a Reineke's diameter of 8 inches would have a cubic volume of about 2,000 cubic feet per acre.

Example Use in Prioritizing Stands for Thinning

The implications of site factors for treatment prioritization can be illustrated by looking at six contrasting examples of stands that would warrant immediate thinning to avoid competition-related mortality (table 1).

Moving from humid to arid sites corresponds with a relatively consistent, proportional restriction of the zone of imminent mortality. In other words, carrying capacity is always lower on arid sites. The effect of Ndep is nuanced across the range of Reineke's diameter. Higher Ndep rates disproportionately lower the zone of imminent mortality for both small- and large-diameter stands. All else being equal, small- and large-diameter stands on arid, polluted sites would warrant prioritization for thinning to avoid competition-related mortality before intermediate-diameter stands on humid, polluted sites.

Table 1—Tree density by nitrogen deposition (Ndep), Reineke's diameter, and annual heat-moisture index (AHM) with a relative density of 60 percent

Stand characteristics	AHM = 10 (humid site)	AHM = 30 (arid site)
	Trees per acre	
Ndep = 2, Reineke's diameter = 4 inches	1,157	997
Ndep = 10, Reineke's diameter = 4 inches	1,071	923
Ndep = 2, Reineke's diameter = 10 inches	299	243
Ndep = 10, Reineke's diameter = 10 inches	347	283
Ndep = 2, Reineke's diameter = 25 inches	65	51
Ndep = 10, Reineke's diameter = 25 inches	43	33

Note: Ndep units are kilograms of N/hectare/year.

Maximum SDI

Establishing a maximum SDI value is important for applications such as establishing specific density targets in thinning treatments. Maximum SDI can also improve mortality modeling in the Forest Vegetation Simulator through customizing the model via the SDIMAX keyword (Van Dyck and Smith-Mateja 2024). A complication of these nonlinear, site-sensitive DMDs is that no single maximum SDI applies to all conditions.

Depending on Reineke's diameter, AHM, and Ndep, maximum SDI varies between 190 and 550. Users can consult figure 2 for maximum SDI values appropriate for different stand structures and sites. Maximum SDI peaks in stands featuring the combination of low AHM, high Ndep, and Reineke's diameters of about 10 inches. Maximum SDI is lowest for stands with high AHM, high Ndep, and Reineke's diameter of 30 inches. This pattern suggests that moderate rates of Ndep may act as a fertilizer in younger, rapidly growing stands (Clark et al. 2019). In contrast, Ndep may act as a stressor in mature, large-diameter stands with limited ecosystem nutrient demands (Latty et al. 2003). Although these estimates are for Zeide's SDI, they would be equivalent to traditional SDI calculated from QMD in even-aged stands.

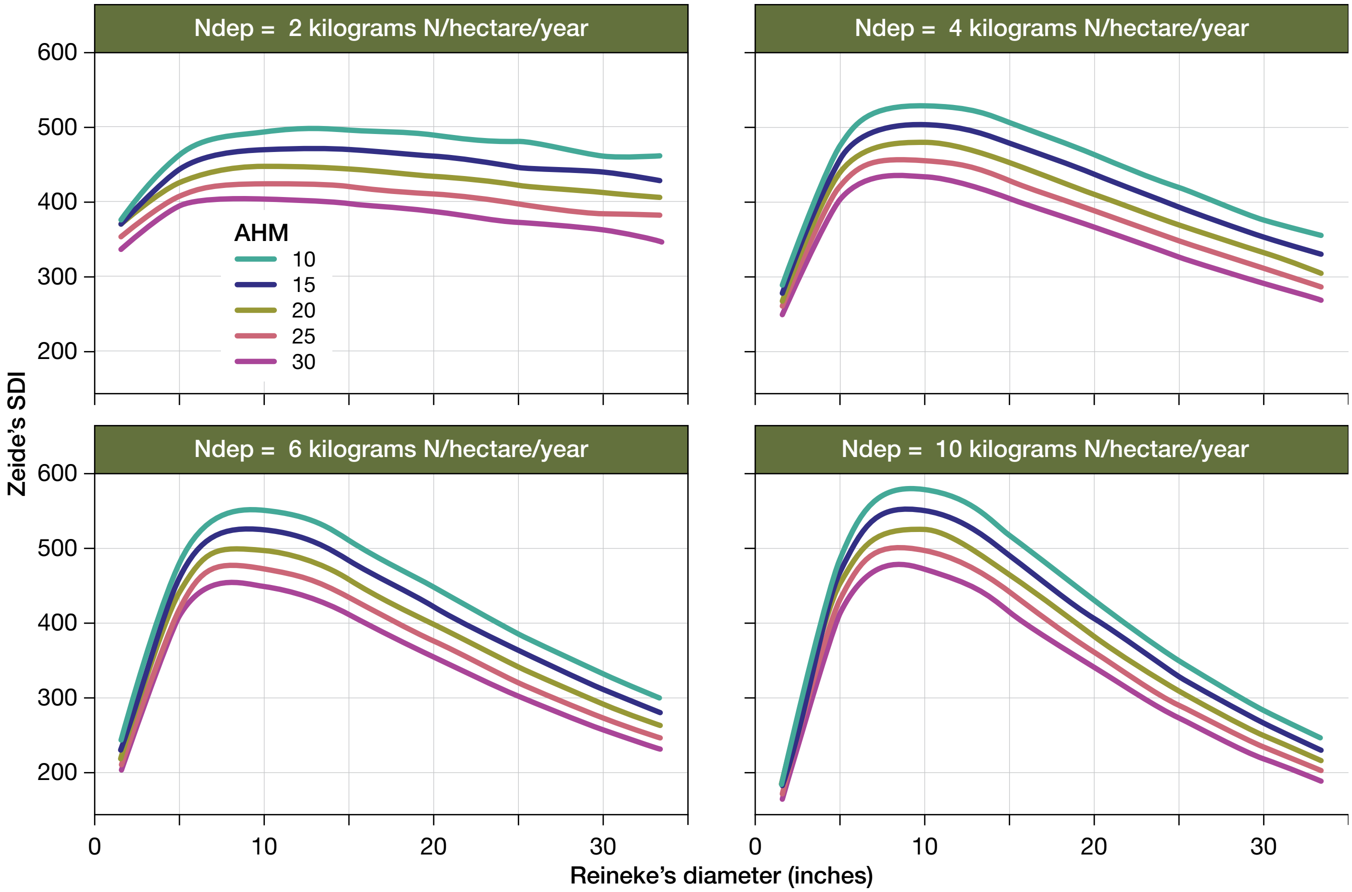

Figure 2—Predicted maximum Zeide's stand density index (SDI) derived from nonlinear density management diagram maximum size-density lines. Line types represent model predictions for discrete values of annual heat-moisture index (AHM). Ndep = nitrogen deposition.

Considering only higher quality sites and Reineke's diameters of about 10 inches, these guidelines are comparable to the overall maximum SDI of 550 that Long and Shaw (2012) reported for California mixed-conifer stands. Otherwise, these guidelines are similar to those for pure, even-aged ponderosa pine stands in California (Zhang et al. 2013). Two factors may account for generally lower maximum California mixed-conifer stocking guidelines in this study compared to Long and Shaw (2012). For this study, I used a more conservative quantile regression, whereas Long and Shaw (2012) used a graphical fitting technique. I also analyzed data following a major regional tree mortality event in the 2010s (Fettig et al. 2019). This drought and bark beetle-driven mortality event likely eliminated many pine-dominated stands that helped define the maximum size-density line before the study by Long and Shaw (2012).

Considerations for Management

These DMDs are equally applicable to young, even-aged stands and mature or uneven-aged stands. In managed forests, maximum stocking guidelines for stands of pole- and sawtimber-sized trees will likely be more relevant than for dense stands of saplings. Under current California forest practices, reforestation has shifted from close-planting spacings to more open densities of ≤200 trees per acre (Stewart 2020). The DMDs can help determine if these widely planted stands require precommercial thinning, or if thinning can be effectively deferred until trees reach commercial size.

As with traditional site-insensitive DMDs for even-aged stands, users applying these tools for designing thinning treatments may wish to keep relative density between 35 and 60 percent of maximum stocking when managing for timber or certain wildlife objectives. However, these guidelines will generally become progressively more restrictive as Reineke's diameter increases. As an example of a potential consequence, consecutive thin-from-below treatments spaced over multiple decades would have successively lower residual absolute density targets as stands mature beyond a Reineke's diameter of 10 inches. In support of these guidelines, Looney and Shaw (2025) found that mortality rates were highest in large-diameter California mixed-conifer stands, which is consistent with large trees being especially vulnerable to loss in regional tree mortality events (Fettig et al. 2019, Koontz et al. 2021). Other drivers of lower maximum stocking in mature stands are the declining ability of lower canopy trees to fully occupy large canopy gaps (Shaw and Long 2007) and declining sapling recruitment (Looney and Shaw 2025).

Historical reconstructions of California mixed-conifer stands inform treatments seeking to reduce hazardous fuels, while restoring ecosystem function (Knapp et al. 2017, Ritchie 2005). North et al. (2022) found that stands subject to an intact, low-severity fire regime commonly did not achieve full site occupancy by even-aged stand guidelines. Yet when plotting the density and QMD of reconstructed stands of sparse, large-diameter trees reported by North et al. (2022) on the DMDs in figures A2.1–A2.5, historical stands more commonly achieved full site occupancy by these new, uneven-aged stand guidelines. A complication is that there have been dramatic rises in Ndep since 1911, when the historical data used by North et al. (2022) were collected, particularly in southern California and the southern Sierra Nevada (Takemoto et al. 2001). As illustrated in the DMDs, higher Ndep disproportionately restricts stocking in contemporary large-diameter stands (Looney and Shaw 2025). Consequently, historical increases in pollution may render these relatively open reference conditions even more relevant to managing large-diameter stands today. For intermediate-diameter stands, the DMDs typically allow thresholds for achieving full site occupancy. However, users may consider balancing stand management guidelines for optimizing stand growth versus reducing fire risk.

Beyond managing the big trees in mature stands, a key consideration is managing regeneration to set the future trajectory of the stand. Looney and Shaw (2025) found evidence of depressed recruitment rates in large-diameter stands. This has negative implications for sustaining stands with large Reineke's diameters but may have positive implications for reduced ladder fuel recovery after thinning (Fialko et al. 2020). When conducting regeneration harvests, evenly distributed stand density reductions that create small gaps (e.g., per single-tree selection or the uniform shelterwood methods) are unlikely to regenerate fire-resistant, shade-intolerant pine species (Brodie et al. 2023, York 2015). Where regeneration of shade-intolerant species is desired, the improved suitability of these DMDs for uneven-aged stands makes them useful for techniques such as group selection, which has been proposed as an effective means for promoting shade-intolerant pine species when combined with prescribed fire and planting (Ritchie 2005, York et al. 2021).

In this study, I used gridded climate and Ndep data to represent site quality. These more direct measures of site quality avoid issues with assessing site index for uneven-aged, mixed-species stands (Skovsgaard and Vanclay 2008). However, these indices do not account for soil fertility or soil water-holding capacity. The latter is particularly critical in California where soil moisture availability is a key control over tree performance and potential species distribution in a Mediterranean climate defined by pronounced summer drought (Flint et al. 2024, Lutz et al.

2010). In terms of application to maximum stocking, previous research has established that soil factors have influences on maximum stocking that are distinct from climate (Heiderman and Kimsey 2021). Future applied research might investigate whether incorporating additional information on soil factors, such as the Basin Characterization Model's (Flint et al. 2013) estimates of site water balance, offers improved site-specific guidelines for managing California mixed-conifer stand density.

Acknowledgments

Thanks to Tom Brandeis, Justin DeRose, and Malcolm North for thorough and constructive informal peer reviews on the manuscript. Nels Johnson provided statistical review and additional helpful comments. Thanks to Melissa Kunz and Arthur "AJ" Moses for additional review, comments, and suggestions on the manuscript.

U.S. Standard Equivalents

When you know:	Multiply by:	To find:
Millimeters	0.0394	Inches
Meters	3.28	feet
Hectares	2.47	Acres
Kilograms	2.205	Pounds
Degrees Celsius (°C)	1.8 °C + 32	Degrees Fahrenheit

Metric Equivalents

When you know:	Multiply by:	To find:
Inches	2.54	Centimeters
Feet	0.305	Meters
Acres	0.405	Hectares
Cubic feet	0.0283	Cubic meters

References

Bartoń, K. 2025. MuMIn: multi-model inference. R package version 1.48.11. https://cran.r-project.org/web/packages/MuMIn/index.html. (August 14, 2025).

Brodie, E.G.; Knapp, E.E.; Latimer, A.M.; Safford, H.D.; Vossmer, M.; Bisbing, S.M. 2023. The century-long shadow of fire exclusion: historical data reveal early and lasting effects of fire regime change on contemporary forest composition. Forest Ecology and Management. 539: 121011. https://doi.org/10.1016/j.foreco.2023.121011.

Brooks, M.; Bolker, B.; Kristensen, K.; Maechler, M.; Magnusson, A.; McGillycuddy, M.; Skaug, H.; Nielsen, A.; Berg, C.; van Bentham, K.; Sadat, N.; Lüdecke, D.; Lenth, R.; O'Brien, J.; Geyer, C.J.; Jagan, M.; Wiernik, B.; Stouffer, D.B.; Agronah, M.; Akdur, H.T.K.; Bové, D.S.; Krieger, N. 2025. glmmTMB: generalized linear mixed models using template model builder. R package version 1.1.12. https://doi.org/10.32614/CRAN.package.glmmTMB. (August 19, 2025).

Buck, J.M.; Adams, R.S.; Cone, J.; Conkle, M.T.; Libby, W.J.; Eden, C.J.; Knight, M.J. 1970. California tree seed zones. San Francisco: U.S. Department of Agriculture, Forest Service, California Region. 5 p. https://research.fs.usda.gov/treesearch/41438. (July 21, 2025).

Burnham, K.P.; Anderson, D.R. 2002. Model selection and multimodel inference: a practical information-theoretic approach. 2nd ed. New York: Springer-Verlag. 488 p.

Burrill, E.A.; DiTommaso, A.M.; Turner, J.A.; Pugh, S.A.; Christensen, G.; Perry, C.J.; Lepine, L.C.; Walker, D.M.; Conkling, B.L. 2024. Forest Inventory and Analysis Database, FIADB user guides, volume database description (version 9.2), nationwide forest inventory. U.S. Department of Agriculture, Forest Service. 1042 p. https://research.fs.usda.gov/sites/default/files/2024-05/wo-v9-2_apr2024_ug_fiadb_database_description_nfi.pdf. (July 21, 2025).

California Department of Forestry and Fire Protection [CAL FIRE]. 2023. California seed zones. https://gis.data.ca.gov/datasets/CALFIRE-Forestry::california-seed-zones/about. (April 6, 2025).

Chivhenge, E.; Ray, D.G.; Weiskittel, A.R.; Woodall, C.W.; D'Amato, A.W. 2024. Evaluating the development and application of stand density index for the management of complex and adaptive forests. Current Forestry Reports. 10(2): 133–152. https://doi.org/10.1007/s40725-024-00212-w.

Clark, C.M.; Richkus, J.; Jones, P.W.; Phelan, J.; Burns, D.A.; de Vries, W.; Du, E.; Fenn, M.E.; Jones, L.; Watmough, S.A. 2019. A synthesis of ecosystem management strategies for forests in the face of chronic nitrogen deposition. Environmental Pollution. 248: 1046–1058. https://doi.org/10.1016/j.envpol.2019.02.006.

Dean, T.J.; Baldwin, V.C., Jr. 1996. The relationship between Reineke's stand-density index and physical stem mechanics. Forest Ecology and Management. 81(1–3): 25–34. https://doi.org/10.1016/0378-1127(95)03666-0.

Ducey, M.J.; Larson, B.C. 2003. Is there a correct stand density index? An alternate interpretation. Western Journal of Applied Forestry. 18(3): 179–184. https://doi.org/10.1093/wjaf/18.3.179.

Dunning, D.; Reineke, L.H. 1933. Preliminary yield tables for second-growth stands in the California pine region. Tech. Bull. 354. Washington, DC: U.S. Department of Agriculture. 24 p. https://research.fs.usda.gov/treesearch/60312.

Fettig, C.J.; Mortenson, L.A.; Bulaon, B.M.; Foulk, P.B. 2019. Tree mortality following drought in the central and southern Sierra Nevada, California, U.S. Forest Ecology and Management. 432: 164–178. https://doi.org/10.1016/j.foreco.2018.09.006.

Fialko, K.; Ex, S.; Wolk, B.H. 2020. Ecological niches of tree species drive variability in conifer regeneration abundance following fuels treatments. Forest Ecology and Management. 476: 118475. https://doi.org/10.1016/j.foreco.2020.118475.

Flint, A.L.; Flint, L.E.; Stern, M.A.; Ackerly, D.D.; Boynton, R.; Thorne, J.H. 2024. Characterizing soil and bedrock water use of native California vegetation. Hydrology. 11(12): 211. https://doi.org/10.3390/hydrology11120211.

Flint, L.E.; Flint, A.L.; Thorne, J.H.; Boynton, R. 2013. Fine-scale hydrologic modeling for regional landscape applications: the California Basin Characterization Model development and performance. Ecological Processes. 2: 25. https://doi.org/10.1186/2192-1709-2-25.

Forrester, D.I.; Baker, T.G.; Elms, S.R.; Hobi, M.L.; Ouyang, S.; Wiedemann, J.C.; Xiang, W.; Zell, J.; Pulkkinen, M. 2021. Self-thinning tree mortality models that account for vertical stand structure, species mixing and climate. Forest Ecology and Management. 487: 118936. https://doi.org/10.1016/j.foreco.2021.118936.

Frescino, T.S.; Moisen, G.G.; Patterson, P.L.; Toney, C.; White, G.W. 2023. 'FIESTA': a forest inventory estimation and analysis R package. Ecography. 2023(7): e06428. https://doi.org/10.1111/ecog.06428.

Gibson, J.; Moisen, G.; Frescino, T.; Edwards, T.C., Jr. 2014. Using publicly available forest inventory data in climate-based models of tree species distribution: examining effects of true versus altered location coordinates. Ecosystems. 17(1): 43–53. https://doi.org/10.1007/s10021-013-9703-y.

Hartig, F. 2024. DHARMa: residual diagnostics for hierarchical (multi-level/mixed) regression models. R package version 0.4.7. http://florianhartig.github.io/DHARMa/. (August 14, 2025).

Heiderman, R.R.; Kimsey, M.J., Jr. 2021. A species-specific, site-sensitive maximum stand density index model for Pacific Northwest conifer forests. Canadian Journal of Forest Research. 51(8): 1166–1177. https://doi.org/10.1139/cjfr-2020-0426.

Hijmans, R.J.; van Etten, J.; Sumner, M.; Cheng, J.; Baston, D.; Bevan, A.; Bivand, R.; Busetto, L.; Canty, M.; Fasoli, B.; Forrest, D.; Ghosh, A.; Golicher, D.; Gray, J.; Greenberg, J.A.; Hiemstra, P.; Hingee, K.; Ilich, A.; Karney, C.; Mattiuzzi, M.; Mosher, S.; Naimi, B.; Nowosad, J.; Pebesma, E.; Lamigueiro, O.P.; Racine, E.B.; Rowlingson, B.; Shortridge, A.; Venables, B.; Wueest, R. 2025. raster: geographic data analysis and modeling. R package version 3.6-32. 10.32614/CRAN.package.raster. (August 19, 2025).

Husch, B.; Beers, T.W.; Kershaw, J.A., Jr. 2002. Forest mensuration. 4th ed. Hoboken, NJ: John Wiley & Sons. 456 p.

Kimsey, M.J., Jr.; Shaw, T.M.; Coleman, M.D. 2019. Site sensitive maximum stand density index models for mixed conifer stands across the Inland Northwest, USA. Forest Ecology and Management. 433: 396–404. https://doi.org/10.1016/j.foreco.2018.11.013.

Knapp, E.E.; Lydersen, J.M.; North, M.P.; Collins, B.M. 2017. Efficacy of variable density thinning and prescribed fire for restoring forest heterogeneity to mixed-conifer forest in the central Sierra Nevada, CA. Forest Ecology and Management. 406: 228–241. https://doi.org/10.1016/j.foreco.2017.08.028.

Koenker, R.; Bassett, G., Jr. 1978. Regression quantiles. Econometrica. 46(1): 33–50. https://doi.org/10.2307/1913643.

Koenker, R.; Portnoy, S.; Ng, P.T.; Melly, B.; Zeileis, A.; Grosjean, P.; Moler, C.; Saad, Y.; Chernozhukov, V.; Fernandez-Val, I.; Maechler, M.; Ripley, B.D. 2025. quantreg: quantile regression. R package version 6.1. https://cran.r-project.org/web/packages/quantreg/index.html. (August 14, 2025).

Koontz, M.J.; Latimer, A.M.; Mortenson, L.A.; Fettig, C.J.; North, M.P. 2021. Cross-scale interaction of host tree size and climatic water deficit governs bark beetle-induced tree mortality. Nature Communications. 12: 129. https://doi.org/10.1038/s41467-020-20455-y.

Latty, E.F.; Canham, C.D.; Marks, P.L. 2003. Beech bark disease in northern hardwood forests: the importance of nitrogen dynamics and forest history for disease severity. Canadian Journal of Forest Research. 33(2): 257–268. https://doi.org/10.1139/x02-183.

Long, J.N.; Shaw, J.D. 2012. A density management diagram for even-aged Sierra Nevada mixed-conifer stands. Western Journal of Applied Forestry. 27(4): 187–195. https://doi.org/10.5849/wjaf.11-036.

Looney, C.E.; Shaw, J.D. 2025. Climate and nitrogen deposition constrain the maximum size-density boundary for mature and old-growth stands. Frontiers in Forests and Global Change. 8: 1566459. https://doi.org/10.3389/ffgc.2025.1566459.

Lutz, J.A.; van Wagtendonk, J.W.; Franklin, J.F. 2010. Climatic water deficit, tree species ranges, and climate change in Yosemite National Park. Journal of Biogeography. 37(5): 936–950. https://doi.org/10.1111/j.1365-2699.2009.02268.x.

Næsset, E. 1997. Determination of mean tree height of forest stands using airborne laser scanner data. ISPRS Journal of Photogrammetry and Remote Sensing. 52(2): 49–56. https://doi.org/10.1016/S0924-2716(97)83000-6.

North, M.P.; Tompkins, R.E.; Bernal, A.A.; Collins, B.M.; Stephens, S.L.; York, R.A. 2022. Operational resilience in Western US frequent-fire forests. Forest Ecology and Management. 507: 120004. https://doi.org/10.1016/j.foreco.2021.120004.

R Core Team. 2025. R: A language and environment for statistical computing. Vienna: R Foundation for Statistical Computing. https://www.R-project.org. (August 14, 2025).

Ray, D.; Seymour, R.; Fraver, S.; Berrill, J.-P.; Kenefic, L.; Rogers, N.; Weiskittel, A. 2023. Relative density as a standardizing metric for the development of size-density management charts. Journal of Forestry. 121(5–6): 443–456. https://doi.org/10.1093/jofore/fvad029.

Reineke, L.H. 1933. Perfecting a stand-density index for even-aged forests. Journal of Agricultural Research. 46(7): 627–638.

Ritchie, M.W. 2005. Ecological research at the Goosenest Adaptive Management Area in northeastern California. Gen. Tech. Rep. PSW-GTR-192. Albany, CA: U.S. Department of Agriculture, Forest Service, Pacific Southwest Research Station. 125 p. https://doi.org/10.2737/PSW-GTR-192.

Schmitz, A.; Sanders, T.G.M.; Bolte, A.; Bussotti, F.; Dirnböck, T.; Johnson, J.; Peñuelas, J.; Pollastrini, M.; Prescher, A.-K.; Sardans, J.; Verstraeten, A.; de Vries, W. 2019. Responses of forest ecosystems in Europe to decreasing nitrogen deposition. Environmental Pollution. 244: 980–994. https://doi.org/10.1016/j.envpol.2018.09.101.

Schwede, D.B.; Lear, G.G. 2014. A novel hybrid approach for estimating total deposition in the United States. Atmospheric Environment. 92: 207–220. https://doi.org/10.1016/j.atmosenv.2014.04.008.

Shaw, J.D.; Long, J.N. 2007. A density management diagram for longleaf pine stands with application to red-cockaded woodpecker habitat. Southern Journal of Applied Forestry. 31(1): 28–38. https://doi.org/10.1093/sjaf/31.1.28.

Skovsgaard, J.P.; Vanclay, J.K. 2008. Forest site productivity: a review of the evolution of dendrometric concepts for even-aged stands. Forestry: An International Journal of Forest Research. 81(1): 13–31. https://doi.org/10.1093/forestry/cpm041.

Stewart, W., tech. ed. 2020. Reforestation practices for conifers in California. Berkeley, CA: University of California. 603 p. https://ucanr.edu/sites/default/files/2020-10/337245.pdf. (August 15, 2025).

Takemoto, B.K.; Bytnerowicz, A.; Fenn, M.E. 2001. Current and future effects of ozone and atmospheric nitrogen deposition on California's mixed conifer forests. Forest Ecology and Management. 144(1–3): 159–173. https://doi.org/10.1016/S0378-1127(00)00368-6.

Tian, D.; Bi, H.; Jin, X.; Li, F. 2021. Stochastic frontiers or regression quantiles for estimating the self-thinning surface in higher dimensions? Journal of Forestry Research. 32(4): 1515–1533. https://doi.org/10.1007/s11676-020-01196-6.

Van Dyck, M.G.; Smith-Mateja, E.E., comps. 2024. Keyword reference guide for the Forest Vegetation Simulator. Rev. Fort Collins, CO: U.S. Department of Agriculture, Forest Service, Forest Management Service Center. 117 p. https://www.fs.usda.gov/fmsc/ftp/fvs/docs/gtr/keyword.pdf.

Wang, T.; Hamann, A.; Spittlehouse, D.; Carroll, C. 2016. Locally downscaled and spatially customizable climate data for historical and future periods for North America. PLoS ONE. 11(6): e0156720. https://doi.org/10.1371/journal.pone.0156720.

Weiskittel, A.R.; Kuehne, C. 2019. Evaluating and modeling variation in site-level maximum carrying capacity of mixed-species forest stands in the Acadian Region of northeastern North America. The Forestry Chronicle. 95(3): 171–182. https://doi.org/10.5558/tfc2019-026.

Wilson, B.T.: Lister, A.J.: Riemann, R.I.: Griffith, D.M. 2022. Forest-type groups for the Forest Inventory and Analysis program. U.S. Department of Agriculture, Forest Service. https://www.arcgis.com/home/item.html?id=86f34e91135b468f9f81787d0c2b72b1. (August 14, 2025).

Yang, S.-I.; Brandeis, T.J. 2022. Estimating maximum stand density for mixed-hardwood forests among various physiographic zones in the eastern US. Forest Ecology and Management. 521: 120420. https://doi.org/10.1016/j.foreco.2022.120420.

York, R.A. 2015. Large-tree removal in a mixed-conifer forest halves productivity and increases white fir. California Agriculture. 69(1): 27–35. https://doi.org/10.3733/ca.v069n01p27.

York, R.A.; Noble, H.; Quinn-Davidson, L.N.; Battles, J.J. 2021. Pyrosilviculture: combining prescribed fire with gap-based silviculture in mixed-conifer forests of the Sierra Nevada. Canadian Journal of Forest Research. 51(6): 781–791. https://doi.org/10.1139/cjfr-2020-0337.

Zeide, B. 1983. The mean diameter for stand density index. Canadian Journal of Forest Research. 13(5): 1023–1024. https://doi.org/10.1139/x83-135.

Zhang, J.; Oliver, W.W.; Powers, R.F. 2013. Reevaluating the self-thinning boundary line for ponderosa pine (*Pinus ponderosa*) forests. Canadian Journal of Forest Research. 43(10): 963–971. https://doi.org/10.1139/cjfr-2013-0133.

Zuur, A.F.; Ieno, E.N.; Walker, N.J.; Saveliev, A.A.; Smith, G.M. 2009. Mixed effects models and extensions in ecology with R. New York: Springer Science+Business Media. 574 p. https://doi.org/10.1007/978-0-387-87458-6.

Appendix 1: Maps

This appendix provides overview maps of California and allows users to identify values of the annual heat-moisture index (fig. A1.3) and nitrogen deposition parameters (fig. A1.4) summarized by seed zone (fig. A1.2) for their project area. These values are used to select the density management diagram and sets of guidelines (app. 2) that are most relevant to their local site conditions.

California mixed-conifer forest type

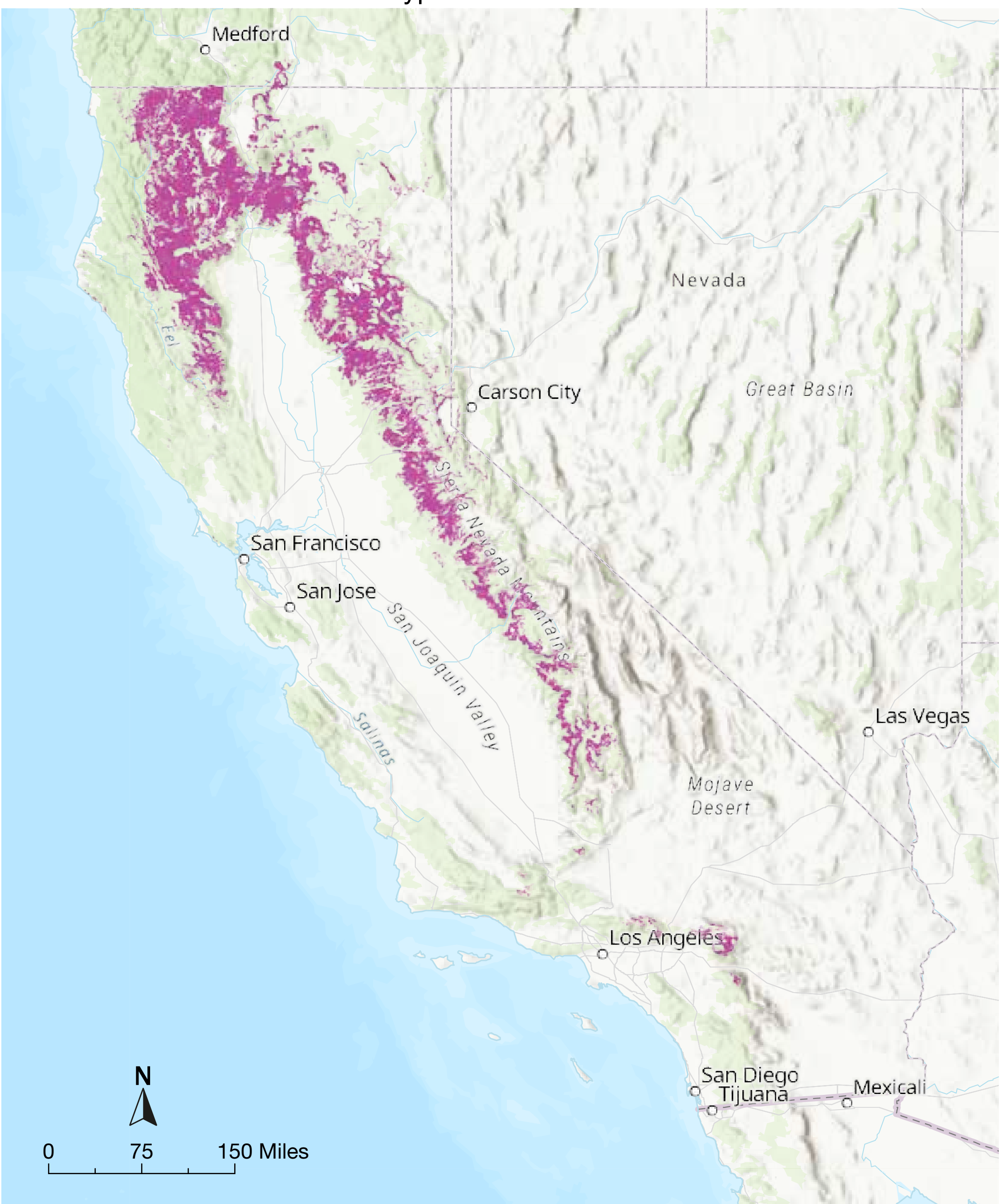

Figure A1.1—Reference map of the California mixed-conifer forest type based on modeled presence/absence data (Wilson et al. 2022).

Figure A1.2—Reference map of California seed zone polygons with probable major occurrences of California mixed-conifer and associated conifer forest types. The numbers on the polygons are the seed zone number (CAL FIRE 2023).

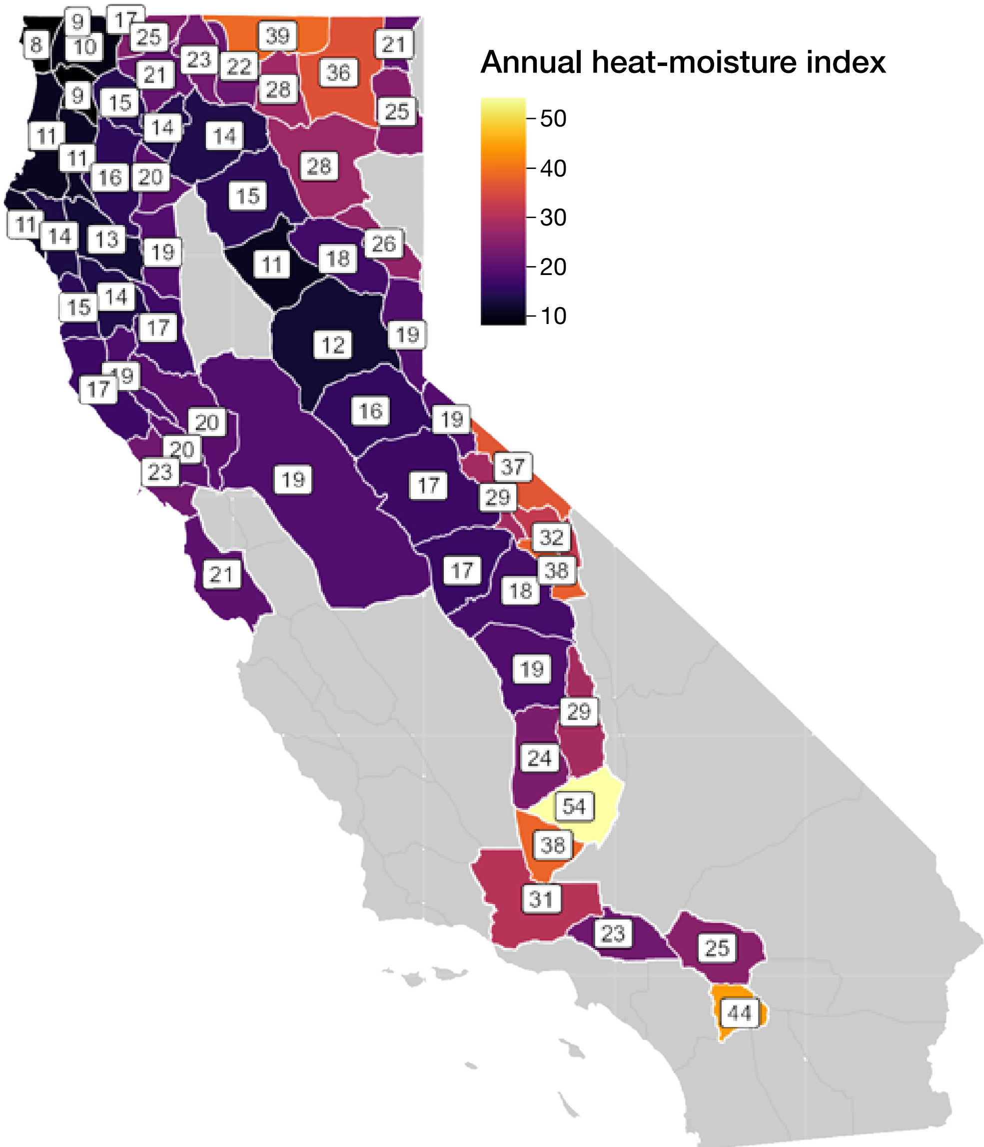

Figure A1.3—Heat map showing the mean annual heat-moisture index (AHM) based on 1991–2020 records summarized by California seed zone. Numbers denote precise values by seed zone.

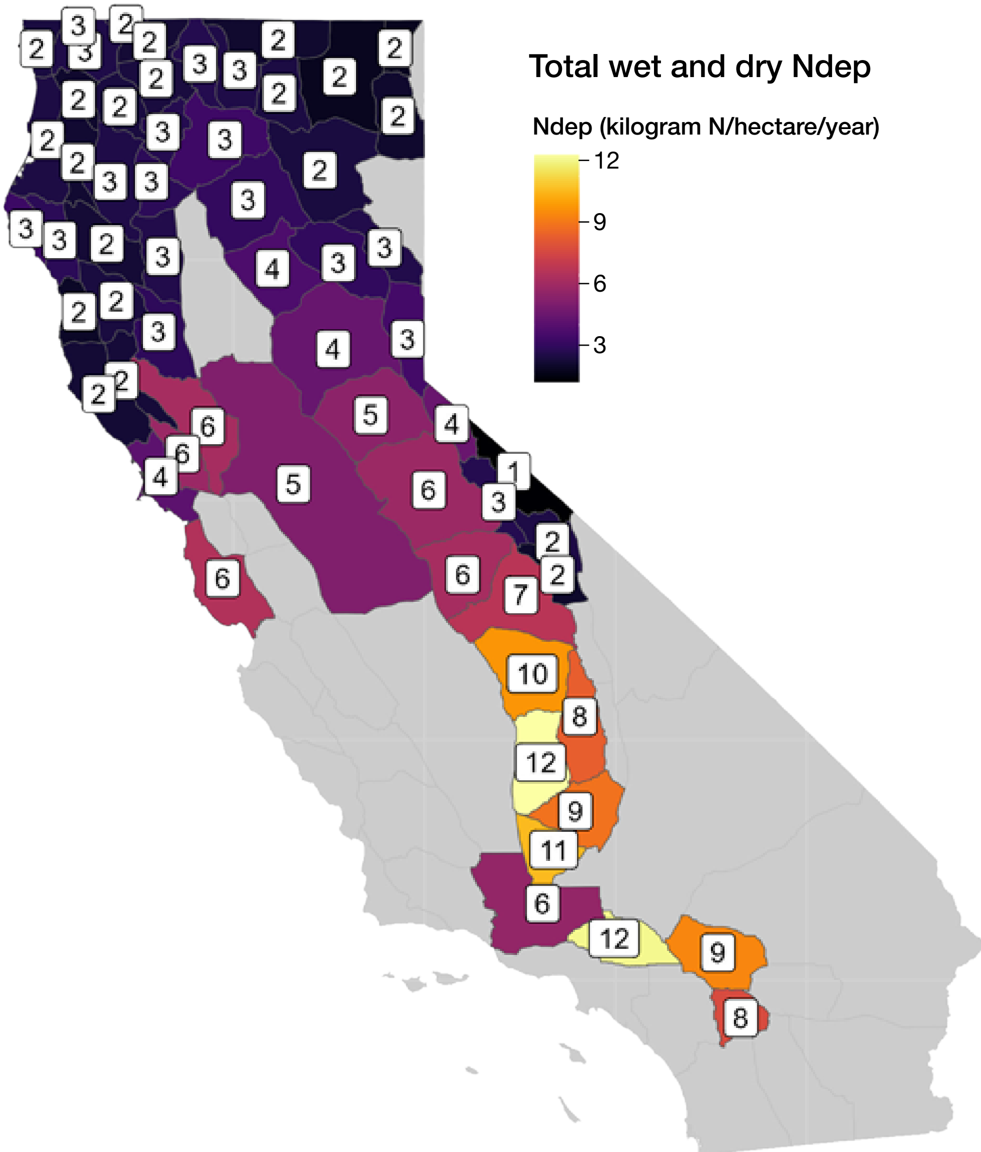

Figure A1.4—Heat map showing the mean total wet and dry nitrogen deposition (Ndep) based on 1991–2020 records and summarized by California seed zone. Numbers denote precise values by seed zone.

Appendix 2: Density Management Diagrams

This appendix provides sets of California mixed-conifer forest type density management guidelines, which flexibly accommodate both even- and uneven-aged stands while accounting for stress from aridity and nitrogen deposition. Users should first select the appropriate density management diagram based on local values of the annual heat-moisture index (fig. A1.3) and then the appropriate set of guidelines based on local values of nitrogen deposition (fig. A1.4).

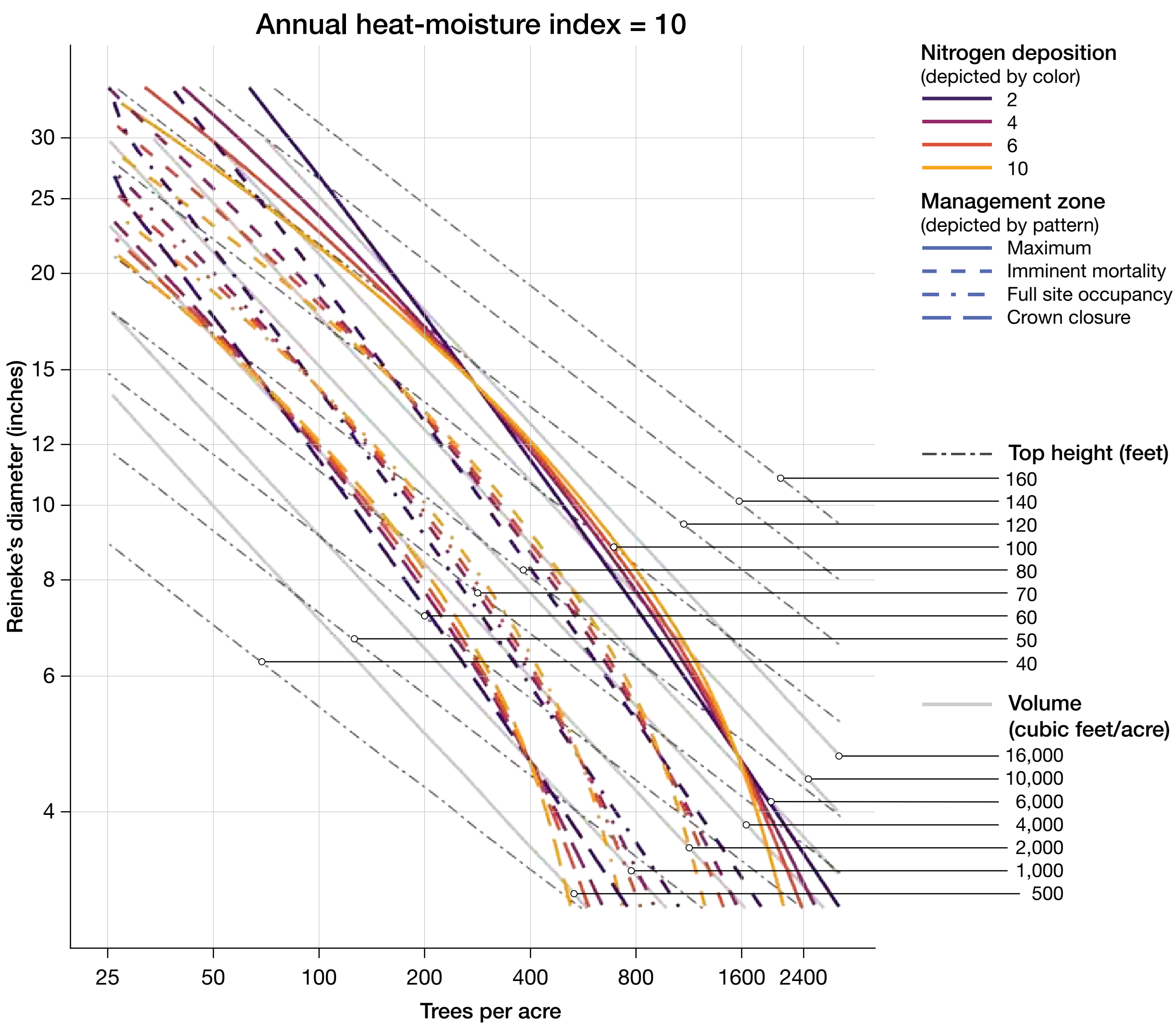

Figure A2.1—Density management diagram depicting management guidelines for humid sites with an annual heat-moisture index of 10. Trees per acre (*x*-axis) and Reineke's diameter (*y*-axis) are log-transformed. Line styles depict the maximum size-density boundary (maximum), threshold of elevated density-dependent mortality (imminent mortality), lower boundary of rapid potential stand growth (full site occupancy), and the onset of inter-tree competition (crown closure). Colors represent discrete values of nitrogen deposition in kilogram/hectare/year. Total volume (cubic feet/acre) is shown with solid gray isolines with leader lines pointing to corresponding values. Top height (feet) is shown with gray dot-dashed isolines with leader lines pointing to corresponding values.

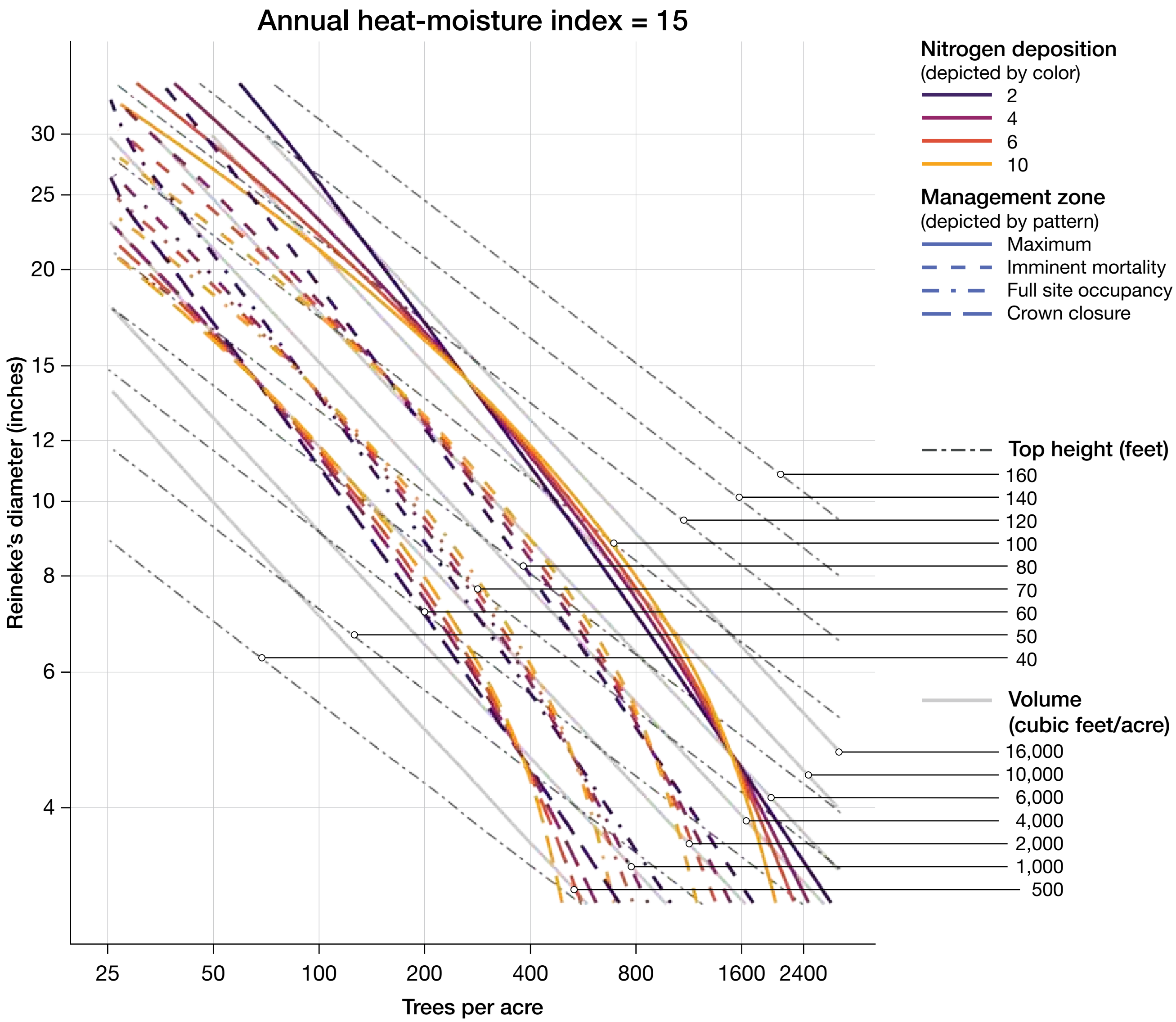

Figure A2.2—Density management diagram depicting management guidelines for moderately humid sites with an annual heat-moisture index of 15. Trees per acre (*x*-axis) and Reineke's diameter (*y*-axis) are log-transformed. Line styles depict the maximum size-density boundary (maximum), threshold of elevated density-dependent mortality (imminent mortality), lower boundary of rapid potential stand growth (full site occupancy), and the onset of inter-tree competition (crown closure). Colors represent discrete values of nitrogen deposition in kilogram/hectare/year. Total volume (cubic feet/acre) is shown with solid gray isolines with leader lines pointing to corresponding values. Top height (feet) is shown with gray dot-dashed isolines with leader lines pointing to corresponding values.

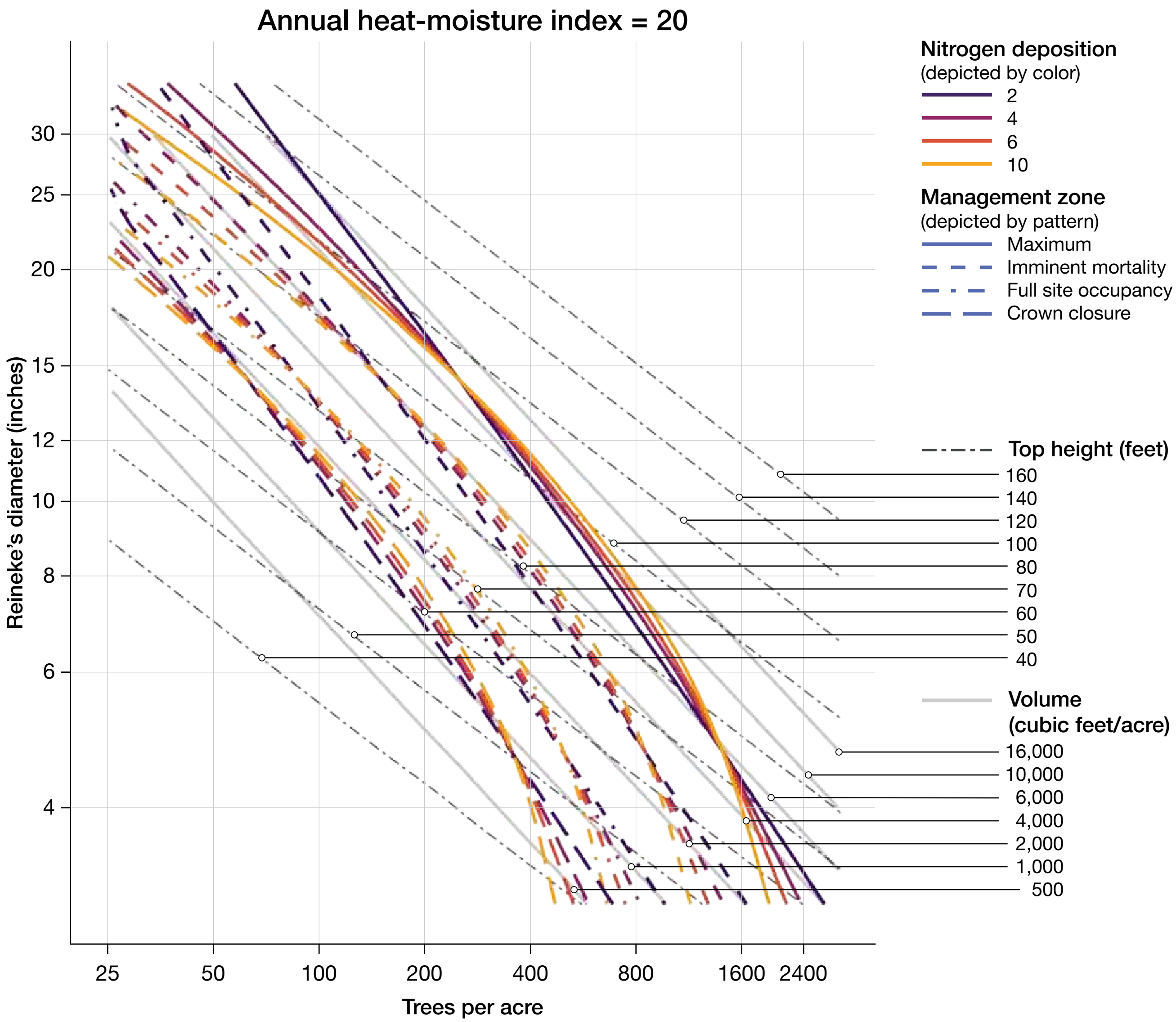

Figure A2.3—Density management diagram depicting management guidelines for intermediate sites with an annual heat-moisture index of 20. Trees per acre (*x*-axis) and Reineke's diameter (*y*-axis) are log-transformed. Line styles depict the maximum size-density boundary (maximum), threshold of elevated density-dependent mortality (imminent mortality), lower boundary of rapid potential stand growth (full site occupancy), and the onset of inter-tree competition (crown closure). Colors depict discrete values of nitrogen deposition in kilogram/hectare/year. Total volume (cubic feet/acre) is shown with solid gray isolines with leader lines pointing to corresponding values. Top height (feet) is shown with grey dot-dashed isolines with leader lines pointing to corresponding values.

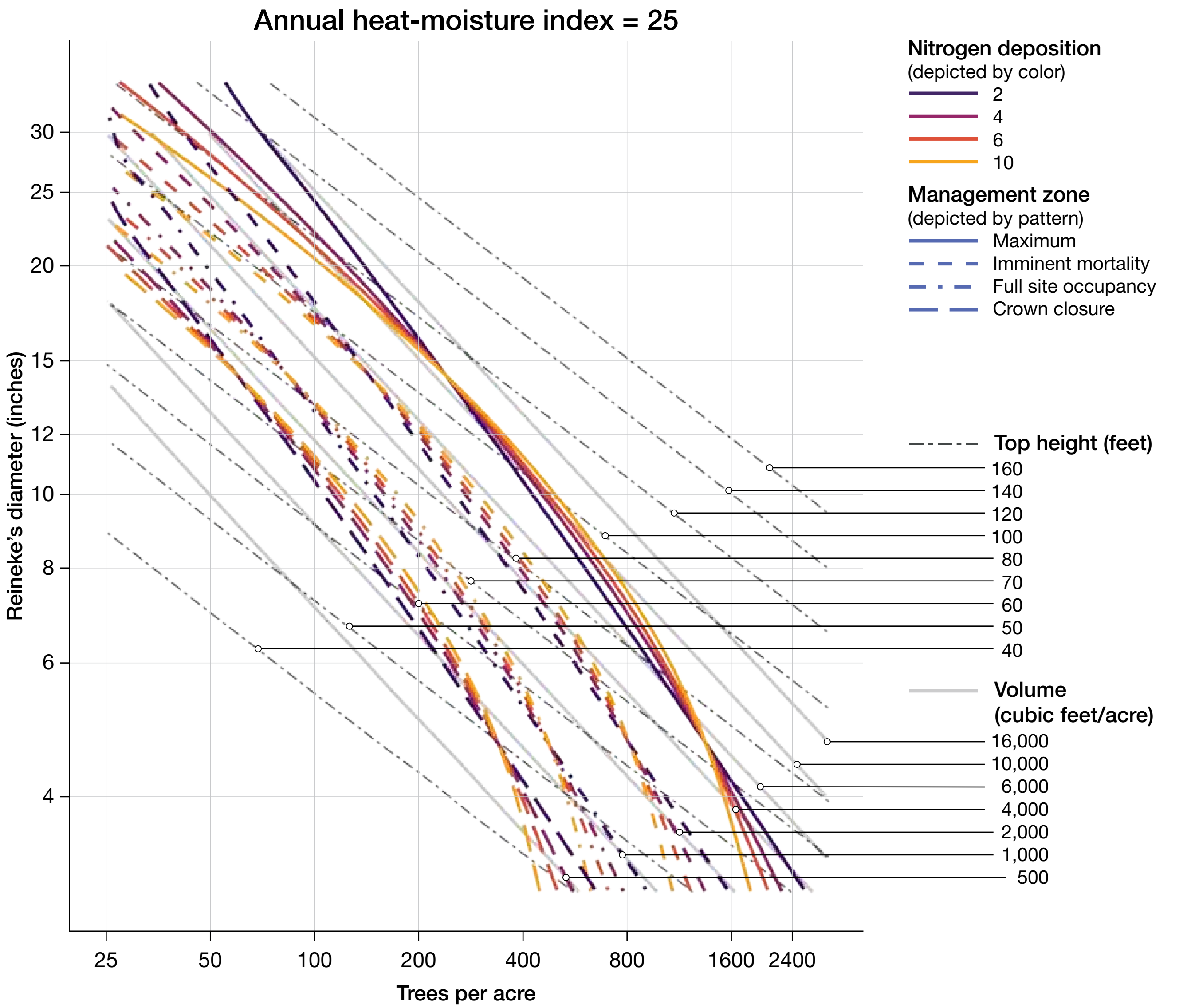

Figure A2.4—Density management diagram depicting management guidelines for moderately arid sites with an annual heat-moisture index of 25. Trees per acre (*x*-axis) and Reineke's diameter (*y*-axis) are log-transformed. Line styles depict the maximum size-density boundary (maximum), threshold of elevated density-dependent mortality (imminent mortality), lower boundary of rapid potential stand growth (full site occupancy), and the onset of inter-tree competition (crown closure). Colors depict discrete values of nitrogen deposition in kilogram/hectare/year. Total volume (cubic feet/acre) is shown with solid gray isolines with leader lines pointing to corresponding values. Top height (feet) is shown with gray dot-dashed isolines with leader lines pointing to corresponding values.

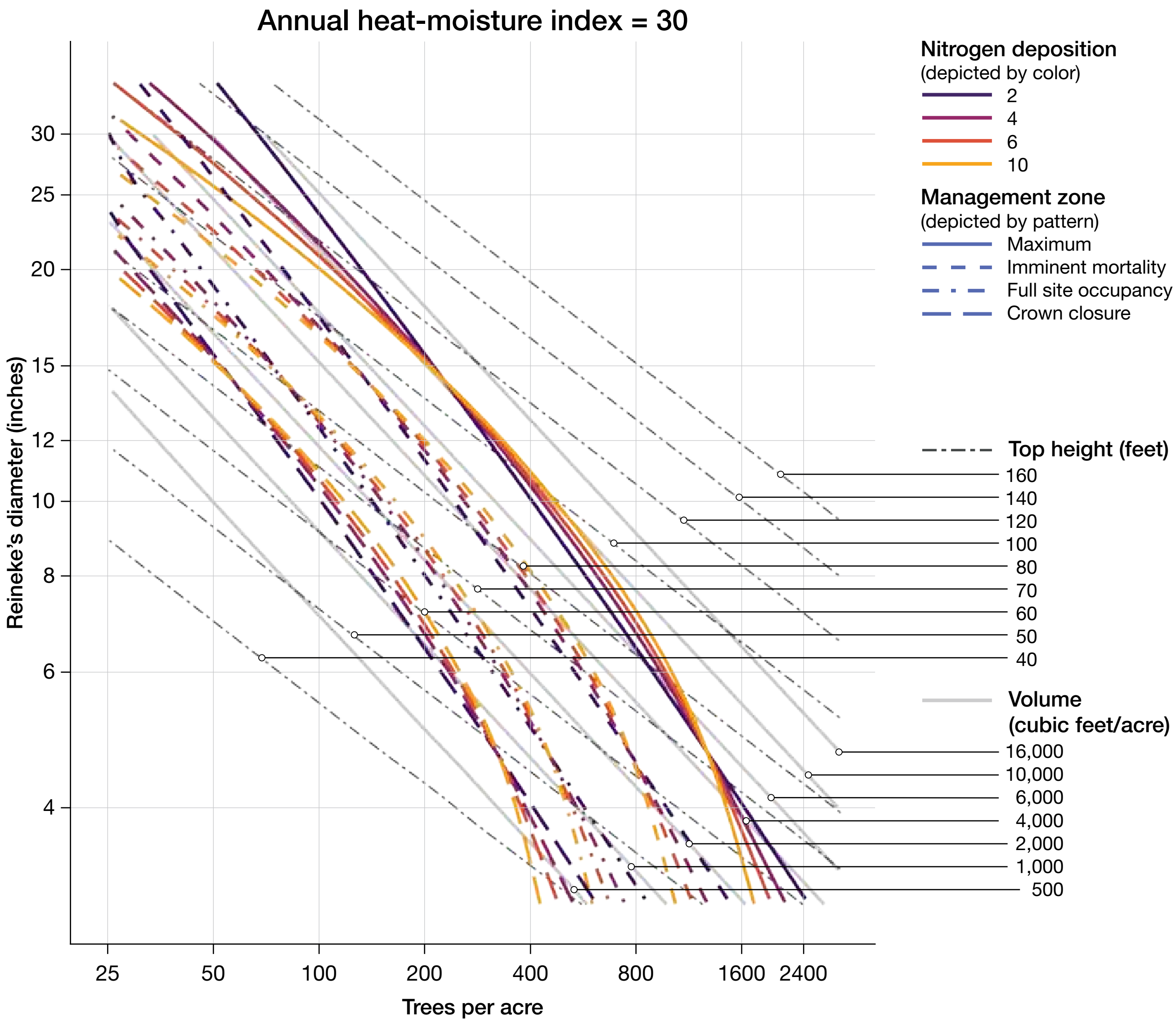

Figure A2.5—Density management diagram depicting management guidelines for arid sites with an annual heat-moisture index of 30. Trees per acre (*x*-axis) and Reineke's diameter (*y*-axis) are log-transformed. Line styles depict the maximum size-density boundary (maximum), threshold of elevated density-dependent mortality (imminent mortality), lower boundary of rapid potential stand growth (full site occupancy), and the onset of inter-tree competition (crown closure). Colors depict discrete values of nitrogen deposition in kilogram/hectare/year. Total volume (cubic feet/acre) is shown with solid gray isolines with leader lines pointing to corresponding values. Top height (feet) is shown with gray dot-dashed isolines with leader lines pointing to corresponding values.

This publication is available online at https://research.fs.usda.gov/psw.

Pacific Southwest Research Station
1323 Club Drive
Vallejo, CA 94592